

**DISAPPEARANCE AND REAPPEARANCE OF PARTICLES OF ENERGIES >50 KEV  
AS SEEN BY P78-2 (SCATHA) AT NEAR GEOSYNCHRONOUS ORBIT\***

**J. Feynman and N. A. Saflekos  
Boston College**

**H. G. Garrett  
Jet Propulsion Laboratory**

**D. A. Hardy and E. G. Mullen  
Air Force Geophysics Laboratory**

SUMMARY

The near-geosynchronous orbit of the P78-2 (SCATHA) satellite is ideal for extending studies of processes earlier detected by the series of geosynchronous vehicles. SCATHA's apogee and perigee are 5.5 and 7.7  $R_E$  and the latitudinal drift is 6° per day. This allows SCATHA to sweep through the geosynchronous region and sample the magnetospheric environment over a widened range of latitude and distance from the earth. A survey of the nightside particle environment as observed by the AFGL Rapid Scan Particle Detector frequently shows large, sudden simultaneous changes in the fluxes of electrons and protons with energies above 50 keV which we refer to as dropouts. An interesting feature of SCATHA dropouts is the quasiperiodic behavior of the particle flux amplitudes which often vary with a period of the order of 15 minutes both during the dropout and after the return. A flux return during eclipse caused a major spacecraft charging event of several kilovolts. Our observations are compared with those reported for other geosynchronous satellites. In agreement with ATS-5, we find a marked dependence in the frequency of occurrence due to an effect of the orbit. ATS-5 experienced few dropouts during quiet geomagnetic conditions. However, for an L shell greater than seven, SCATHA particle dropouts occur routinely during quiet conditions. Thus, for SCATHA's orbit, both the orbital position and geomagnetic conditions must be taken into account in evaluating the potential hazard of flux returns.

---

\*This work was supported in part by Air Force Geophysics Laboratory Contract F19628-79-C-0031.

## INTRODUCTION

On the night side of the earth in geosynchronous orbit, there are frequent sudden disappearances and reappearances of fluxes of electrons and ions in the  $E > 50$  keV energy range (Lezniak and Winckler, 1970, Bogott and Mozer, 1973, Walker et al, 1976). These flux changes, called dropouts, are usually ascribed to the satellites exiting and reentering the region of high energy trapped particles that characterize this part of the magnetosphere.

Here we are primarily concerned with the occurrence of these particle dropouts as experienced by P78-2 (SCATHA) in a near-geosynchronous orbit. Transitions between regions of such high and low fluxes of particles represent one of the most dramatic rapid changes of charging environment routinely present in this orbit. For example, on March 28, 1979 (Day 87) SCATHA was already in a dropout region when it entered eclipse. An abrupt return of plasma during the eclipse caused charging of several kilovolts (Saflekos et al., 1980), one of the major charging events seen on SCATHA during the first year of operation. The rapid variations in the fluxes associated with dropouts imply rapid variations in satellite potential. If, in addition, there are high field aligned fluxes at this boundary, as the data suggest, the possibility exists for creating large differential gradients in the spacecraft potential on the satellite surface. As dropouts occur preferentially in the midnight sector (Walker et al., 1976) eclipses of the satellite are likely to occur simultaneously with the dropouts. During the first eclipse season, dropouts were present during a third of the eclipses that lasted more than 45 minutes. Taken together, the the rapid variation in environment, the flux anisotropies, and the possibility of a simultaneously occurring eclipse, cause the region of the magnetosphere in which dropouts occur to pose a severe spacecraft charging threat. The characterization of this region is necessary for a complete understanding of spacecraft charging variations in and near the midnight sector.

For geosynchronous orbit, Lezniak and Winckler (1970) mention such events as seen by ATS-1. Bogott and Mozer (1973) studied an extensive data set from ATS-5 and explained the disappearances as due to the satellite exiting the region of high energy trapped particles because of the distortion of the region towards a more taillike configuration occurring during substorm buildup. This picture is confirmed by a multi-satellite study (Wilken, et al., 1979). The reappearance of the plasma is then due to the relaxation of the nightside magnetosphere during the expansion phase of substorms. Bogott and Mozer (1973) found the events occurred preferentially at higher levels of geomagnetic activity during summer. The seasonal effect was explained as due to the orbit since ATS-5 is at a position closer to the edge of the trapping region in the summer months than in winter. The geomagnetic effect is in agreement with the picture in which the trapped particle region moves earthward during disturbed periods. The relation between sudden flux changes at synchronous orbit and substorms has been studied by Erickson et al. (1979) and Sauvaud and Winckler (1980). It has also been noted that the boundary often undergoes large scale motions which

appear to be due to traveling waves (Kaufman et al., 1972, Su et al., 1976 Wilken et al., 1979) but that effect is outside the scope of this paper. Here we discuss the positions of occurrence and dependence on geomagnetic disturbance of dropouts as seen at SCATHA's near geosynchronous orbit.

## OBSERVATIONS

The data used in this study are from the SCATHA Rapid Scan Particle Detector, SC5, which is sensitive to electrons in the range from 0.05 keV to 1 MeV and positively charged particles from 0.05 keV to 6 MeV. The detectors and their operation are described in detail in the paper by Hanser et al. (1980) presented at this conference. The instrument consists of two sets of detectors, one mounted with the look direction along the spin axis of the vehicle and the other mounted on the belly band with the look direction perpendicular to the spin axis. In this study, data from only the former are used. Each detector set consists of two parts, electrostatic analyzers for electrons and ions of energies below 60 keV and solid state detectors for the higher energy electrons and protons. Complete spectra composed of 14 energy bands for electrons and 18 energy bands for positively charged particles are taken every second. A data format is used in this study in which minute averages of the count rate in each energy range is displayed for the detector with the look direction parallel to the vehicle spin axis.

Dropouts have been identified from the data as shown in Figure 1 which gives the 100 keV electron and 125 keV ion count rate from the solid state detectors for parts of three days. In the top panel, data from March 28, 1979 show the dropout and return during eclipse on the lefthand side of the figure where the electron flux changes by more than three orders of magnitude and the ion flux by two. This dropout occurred at 22:45 local time when  $K_p = 5-$  and SCATHA was at a solar magnetic latitude of  $-19^\circ$  and an L shell of 7. The L shell is calculated using an Olson Pfitzer (1974) magnetic field model for quiet days. For about an hour after the return to high flux levels, the electrons show intensity excursions as large as an order of magnitude. The count rate gradually decreased over the next several hours until it sank below detectable levels at about 02:30 LT when  $K_p = 3$  and the vehicle was at a latitude of  $-15^\circ$  and an L shell of 8.2. A second recovery occurred at about 04:00 LT and was followed by a remarkable set of apparently quasi-periodic variations in both the electron and ion flux.

The dropouts on March 28 are in contrast to the typically featureless behavior of the nightside 100 keV electron and 125 keV positively charged particle count rate shown in the second panel of Figure 1. These data are from the period spanning midnight GMT between July 31 and August 1, 1979. It was a geomagnetically quiet time with  $K_p$ 's of 1 and 2 and at midnight GMT SCATHA was at a latitude of  $8^\circ$  SM and an L shell of 8.3. The third panel of Figure 1 shows an example of a dropout in which both the flux decrease and increase were rapid. The typical quasiperiodic flux variations are seen over a wide energy range of particles both within the dropout region

and following recovery. The latitude at entry entry was  $10^\circ$  SM, the L shell was 8.6 and Kp 3+. Three other dropouts which occurred during this passage of the nightside are not shown.

The SC5 data for the period between January 20 and August 8, 1979 were examined for dropouts. The 100 keV electron data were scanned for decreases and/or increases of over an order of magnitude in count rate. Then the event was identified as a dropout if the increase or decrease occurred at the same time in all higher electron energies and in all positive particle energies above some threshold. A return from a dropout can be readily distinguished from a dynamic injection seen by SC5 (Moore et al., 1981) by several properties. The dropout return is characterized by a minimum energy above which the increase in flux increases with energy for all energies. The dynamic injection is also characterized by a minimum energy for flux increase but there is a larger energy above which the change in flux decreases with increasing energy. In addition, dropout entry and return occur in both charge species at the same time whereas injections are seen only in one species over a broad energy range.

Comparisons of particle spectra before, during and after a dropout are shown in figures 2 for electrons and 3 for ions. The dropout for which these are taken is shown in the third panel of Figure 1. The relative differential flux is given for the energy range in which the flux is above background during the dropout. Relative flux levels are used in place of absolute flux levels because the efficiency of the instrument determined by in-flight calibration is not yet available for this period. The spectra are determined for 1:30 GMT, well before the dropout, for 3:30 GMT during the dropout and for 4:30 GMT after the positive particle quasiperiodic variations had ceased. The electron spectra in Figure 2 show a dropout spectrum that is depressed by a factor of 2 at 1 keV and a factor of 100 at 40 keV. The electron flux after the dropout is somewhat higher than before the dropout for most of the energy range. Figure 3 shows the ion spectra. The spectrum during dropout is depressed by a factor of 3 at a few keV and by a factor of 20 at 50 keV. The flux at 125 keV is definitely higher than would be expected. Inspection of the data shows the flux level at 125 keV is at a maximum in the quasiperiodic variation in the flux at 3:30 whereas flux levels at lower energies are from minima. The flux minimum at 125 keV is a factor of 10 lower as can be seen in Figure 1. The quasiperiodic structure, then, involves a spectral change, perhaps due to the motion of a dispersed boundary of the high energy trapping region. The positive particle differential flux is almost indistinguishable before and after the dropout and only one line has been drawn in the figure. The stability of the positive particle spectrum is of note when it is recalled that the observations were separated 3 hours in universal time and SCATHA has moved over  $2 R_E$  along its orbit and is half an  $R_E$  further above the equatorial plane during the later measurement.

## MAGNETOSPHERIC POSITION DEPENDENCE OF DROPOUTS

Eight-eight days of SC5 data for the 5 1/2 month period between January 20 and August 8, 1979 were scanned and one or more dropouts identified for 39 of them. The distribution of dropout days in the year is given in two displays in Figure 4. In the bottom panel we show for each 20 day interval the number of dropout days as a percentage of all days for which the data are available. The total number of days with data is given above each 20 day bin. There are three periods during which more than half the days showed dropouts, between days 80 and 100, days 120 and 150 and days 180 and 210. The top panel shows details of the distribution of dropout days. Each day for which the data were available is marked by a line. A short line indicates there was no dropout whereas a long line indicates dropout days. The three dropout rich periods are evident. This clustering into dropout rich and poor periods corresponds to a position dependence in occurrence of dropouts since SCATHA drifts in latitude by  $6^\circ$  a day and has an apogee of 5.5 Re and a perigee of 7.7 Re.

The positions of dropouts are displayed explicitly in Figures 5 and 6. In each of these figures the position of the satellite during the low flux periods is shown as a solid line. The top panels give the L shell and local time whereas the lower panel gives the solar magnetic latitude and local time. Data for flux decreases when  $K_p < 4+$  are shown in Figure 5 and data for  $K_p > 4+$  are in Figure 6. For all dropouts except one, a categorization on the basis of  $K_p$  at flux return would have placed the dropout in the same group as did the categorization on the basis of flux disappearance. The sole exception was a disappearance at  $K_p = 4+$  and a return at  $K_p = 5-$ , and this dropout appears within the clustering apparent in Figure 5. Note that all of the dropouts except one occur between 19:30 LT and 6:30 LT. The dropout beginning at 6:20 LT and continuing to 7:50 shown in Figure 6 occurred when  $K_p$  was 8 and may have been either a dropout or a passage into the magnetosheath. A data gap in our low energy coverage makes it impossible to distinguish between these possibilities. The local time region of dropout appearance shown here agrees with those of ATS-5 and ATS-6, both of which observed dropouts in the region from from 2000 LT to 0830 LT (Bogott and Mozer, 1973; Su et al., 1976). Note that  $L > 7$  for all but 6 dropouts. There is also a region in the vicinity of  $-5^\circ$  SM latitude in which there are no dropouts. The shape of this region is not completely determined, but in this data set it appears to be centered at 1:30 LT and to be about  $10^\circ$  wide. It can be described as oval shaped with a more or less constant width crossing the latitude  $0^\circ$  line at about 05:30 local time and remaining below latitude  $0^\circ$  throughout the evening hours.

Figures 5 and 6 indicate that dropouts are rare during the months of February through August in a region of the magnetosphere bounded by local time 19:30 and 6:30, by L values of about 7 and by the edges of the  $10^\circ$  crescent in solar magnetospheric coordinates discussed above. If this is the case, the orbit of SCATHA during the three dropout poor periods, (before day 80, from day 100 to 120 and from day 150 to 180), should have a relationship to the excluded region of the magnetosphere. In Figure 7 we

show SCATHA's orbit between local times of 19:30 and 6:30 for days 50, 110 and 170. An examination of these orbits show that they lie almost completely within the excluded region. Hence, the division of SCATHA days into dropout rich and poor periods can be understood as a consequence of its orbit and the shape of the region of high energy particle trapping.

#### GEOMAGNETIC DISTURBANCE DEPENDENCE OF DROPOUTS

A very marked dependence of dropout frequency on geomagnetic activity was found for ATS-5 data (Bogott and Mozer, 1973). Walker et al. (1976) observed 75 ATS-6 dropouts for  $K_p < 4+$  in 4.5 months of data and state that this frequency is higher than that seen for ATS-5. They ascribe the frequency difference to ATS-6 being at the higher magnetic latitude but do not discuss the orbital differences in detail.

In the SCATHA data when the satellite was less than  $6.6 R_E$  (not L shell) from the earth, there were only five dropouts for which  $K_p < 4+$  and nine for which  $K_p > 4+$ . Thus, during the first half of 1979 a geosynchronous satellite would have observed few dropouts but would have reported a geomagnetic dependence in occurrence. At the actual SCATHA orbit, the dependence on geomagnetic activity is less pronounced. Figure 4 shows that dropouts were a common occurrence for  $K_p < 4+$ , but they occur at high L shells (and large values of R). A statistical analysis confirms the impression given by Figures 4 and 5, that at SCATHA's orbit, the dropout occurrence probability exhibits a geomagnetic and an orbital dependence which are comparable. In Table 1 the data has been divided into two sets of periods. The one set contains the dropout rich periods, days 81 to 100, 121 to 149 and 181 to 220, whereas the other set contains the dropout poor periods, days 40 to 80, 100 to 120 and 150 to 180. Each set of data is shown separately in the table. Geomagnetic activity as measured by  $A_p$  has been divided into three bins; quiet days with  $A_p$  0 to 9, (daily average three hours  $K_p < 2$ ) moderate days with  $A_p$  10 to 29 ( $2 < K_p < 4$ ) and disturbed days with  $A_p$  greater than 30 ( $K_p > 4$ ). In the dropout poor set, there were a total of 43 days with data of which three had dropouts. In the 45 days of the dropout rich set, 9 had no dropouts. Thus, if a prediction of dropout occurrence were made using only information on whether the day belonged to a dropout poor or rich region, and taking no account of the level of geomagnetic activity, the correct prediction would have been made for about 6 out of 7 days. Conversely, if the prediction had been made based on distinguishing only between quiet ( $A_p < 9$ ) and disturbed ( $A_p > 30$ ) days and taking no account of dropout poor and rich periods, the correct prediction would have been made in 2 out of 3 days. This indicates that at SCATHA's orbit both the details of the orbital position and the geomagnetic conditions must be taken into account in evaluating the probability that the spacecraft will undergo the extreme environmental changes associated with disappearance and return of high energy trapped particle fluxes.

## SUMMARY AND CONCLUSIONS

At SCATHA's orbit on the nightside, the satellite routinely exits and reenters the region of trapped high energy particles. Since these events occur predominantly near midnight and so may be associated with an eclipse, the flux returns pose a serious charging hazard. ATS-5, ATS-6 and SCATHA all report dropouts occurring from 2000 LT to 08:30 LT. SCATHA experiences dropouts predominantly beyond  $L = 7$  and outside of a region about  $10^\circ$  wide in solar magnetic latitude. The probability of SCATHA dropouts occurring during a particular day has a comparable dependence on both its orbital position and on the level of geomagnetic activity.

## REFERENCES

1. Bogott, F.H. and F.S. Mozer: Nightside Energetic and Particle Decreases at the Synchronous Orbit. *J. Geophys. Res.*, 78, 1973, p. 8119.
2. Erickson, K.N.; R.L. Swanson; R.J., Walker; J.R. Winckler: A study of Magnetospheric Dynamics During Auroral Electrojet Events by Observations of Energetic Electron Intensity Changes at Synchronous Orbit. *J. Geophys. Res.* 84, 1979, p. 931.
3. Hanser, F.A.; B. Sellers; D.A. Hardy; H.A. Cohen, J. Feynman and M.S. Gussenhoven: Operation of the SC5 Rapid Scan Particle Spectrometer on the SCATHA Satellite. Presented at the Spacecraft Charging Technology Conference III.
4. Kaufmann, L.R., J.T. Horng, and A. Konradi: Trapping Boundary and Field Line Motion During Geomagnetic Storms. *J. Geophys. Res.*, 77, 1972, p. 2780.
5. Lezniak, T.W. and J.R. Winckler: Experimental Study of Magnetospheric Motions and the Acceleration of Energetic Electrons During Substorms. *J. Geophys. Res.*, 75, 1970, p. 7075.
6. Moore, T.E., R.L. Arnoldy, J. Feynman and D.A. Hardy: Propagating Substorm Injection Fronts, submitted *J. Geophys. Res.*, 1981.
7. Olson, W.P. and K.A. Pfitzer: A Quantitative Model of the Magnetospheric Magnetic Field. *J. Geophys. Res.*, 79, 1974, p. 3739.
8. Saflekos, N.A.; M. F. Tautz; A.G. Rubin; D.A. Hardy; P.F. Mizera and J. Feynman: Three Dimensional Analysis of Charging Events on Days 87 and 114, 1979 from SCATHA. Presented at Spacecraft Charging Technology Conference III, 1980.
9. Su, Shin-Yi,; T.A. Fritz and A. Konradi: Repeated Sharp Flux Dropouts Observed at 6.6 Re During a Geomagnetic Storm: *J. Geophys. Res.* 81, 1976, p. 245.

10. Walker, R.J., K.N. Erickson, R.L. Swanson, and J.R. Winckler: Substorm-Associated Particle Boundary Motion at Synchronous Orbit. J. Geophys. Res. 81, 5541, 1976.
11. Wilken, B., A. Korth, G. Kremser and Th.A. Fritz: Multiple-Satellite Observations of Large Scale Trapping Boundary Motions. Proceedings of Magnetospheric Boundary Layers Conference, Alpbach, 11-15 June, 1979, ESA SP-148, 1979.

TABLE 1

Periods of few dropouts (days 40-80, 100-120, 150-180)

Range of $A_p$	0-9	10-29	> 30	$\Sigma$
# of dropout days	0	1	2	3
# of no dropout days	17	19	4	40
Total # of days	17	20	6	$\Sigma$ 43

Periods with many dropouts (days 81-100, 121-149, 181-220)

Range of $A_p$	0-9	10-29	> 30	$\Sigma$
# of dropout days	7	20	9	36
# of no dropout days	6	3	0	9
Total # of days	13	23	9	$\Sigma$ 45

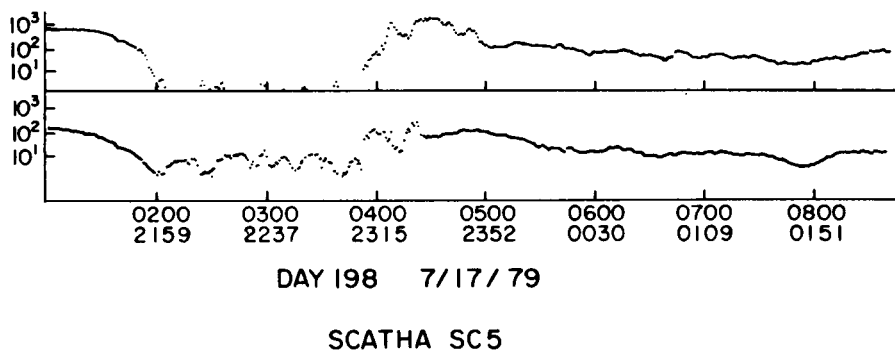
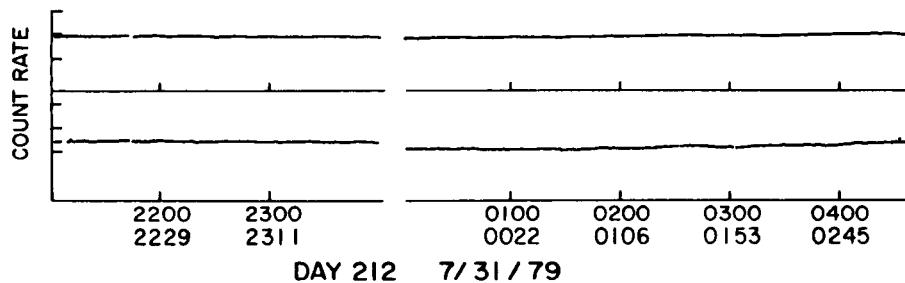
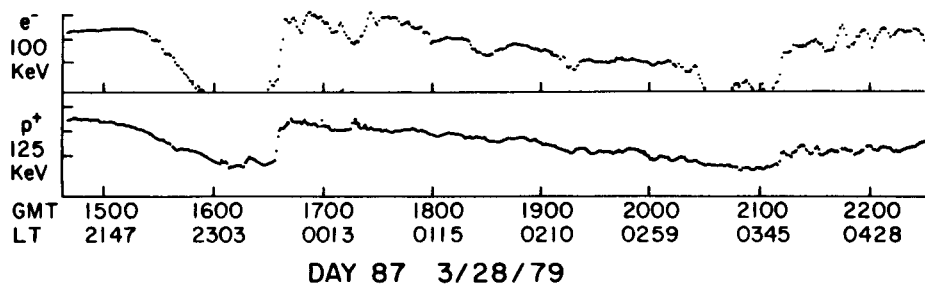


Figure 1. - Dropouts as seen in 100 keV electrons and 125 keV protons by the Rapid Scan Particle Detector, SC5. The first and third panels show dropouts and their characteristic quasiperiodic structures. The center panel contrasts this to a day without dropouts.

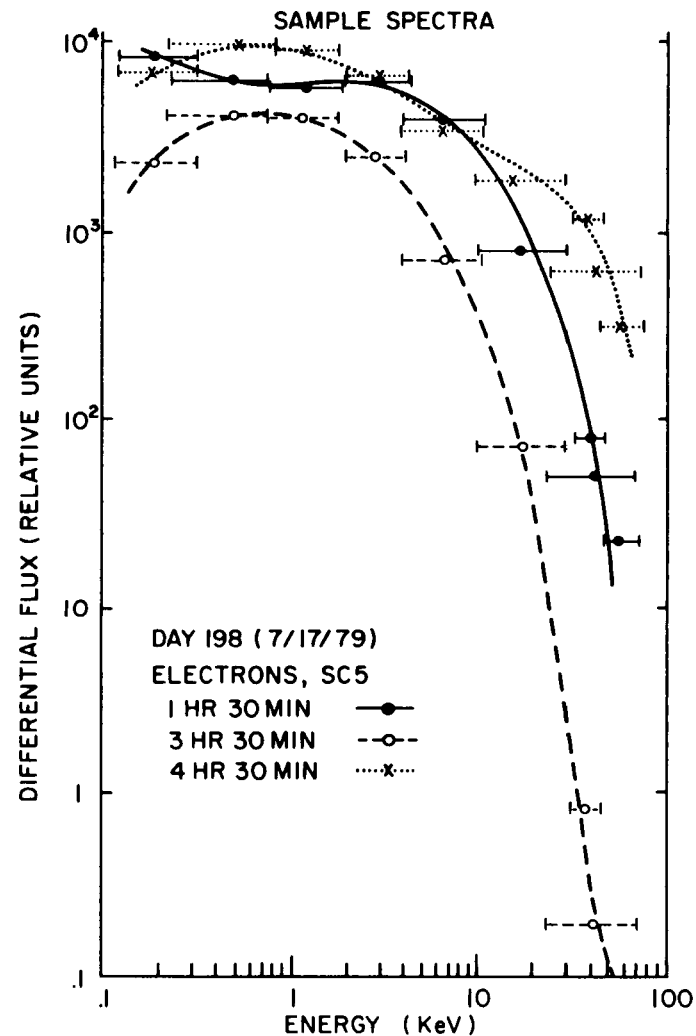


Figure 2. - Electron differential flux before, during and after the dropout shown in the lower panel of Figure 1.

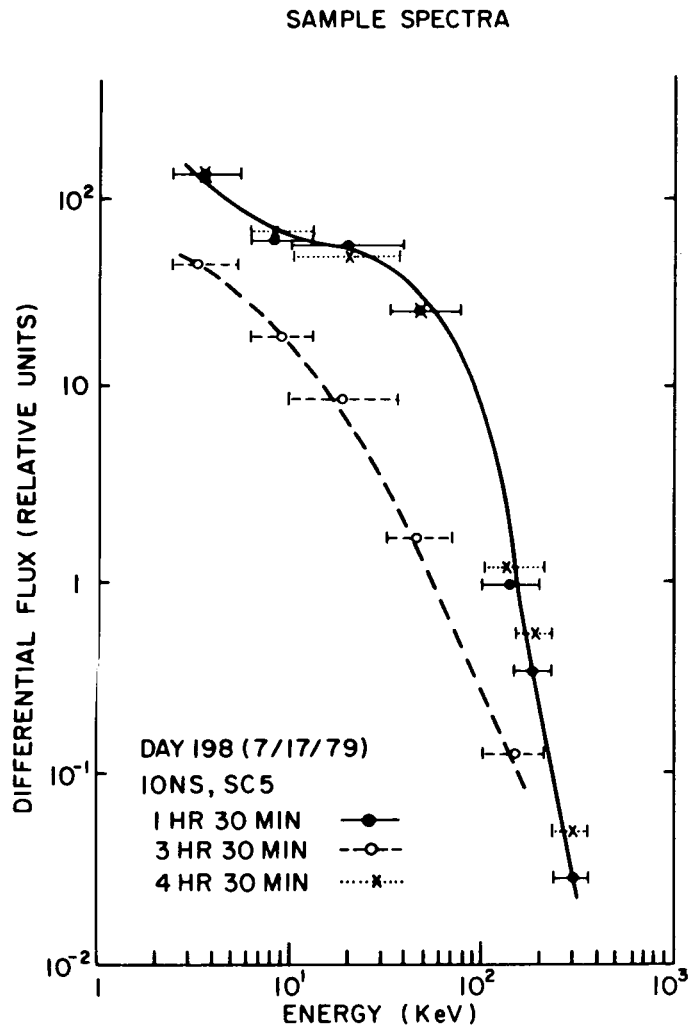


Figure 3. - Ion differential flux before, during and after the dropout shown in the lower panel of Figure 1.

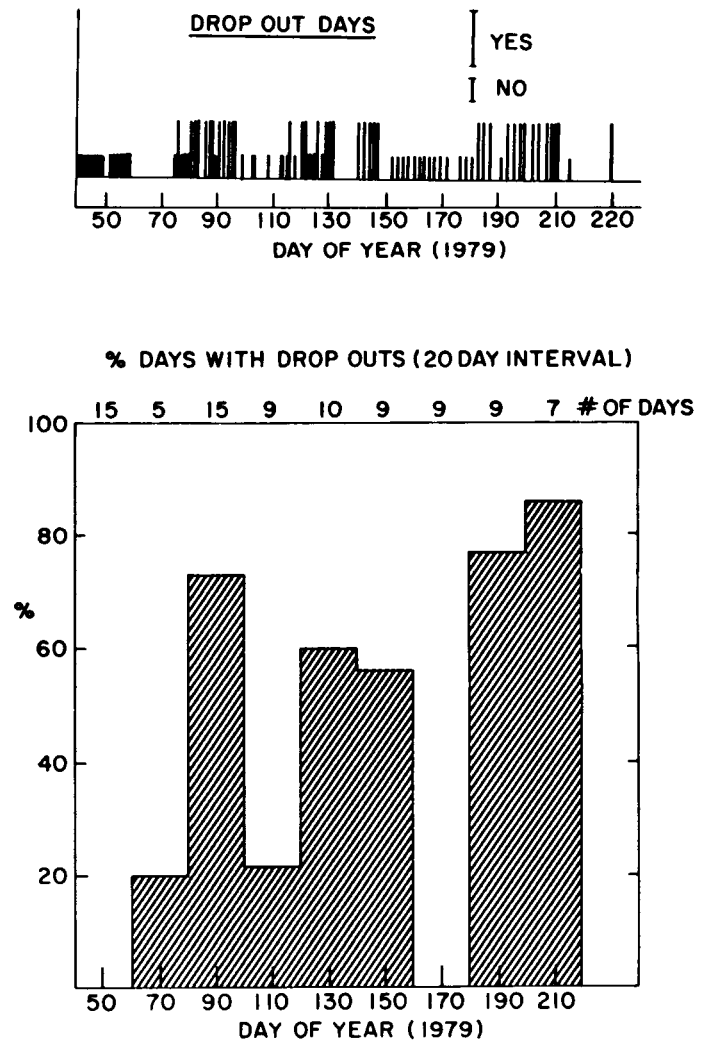


Figure 4. - Dropout occurrence between days 40 and 220, 1979. In the top panel all days for which there are data are labeled according to whether or not dropouts occurred. The percentage of days with dropouts in each 20 day interval is shown in bottom panel.

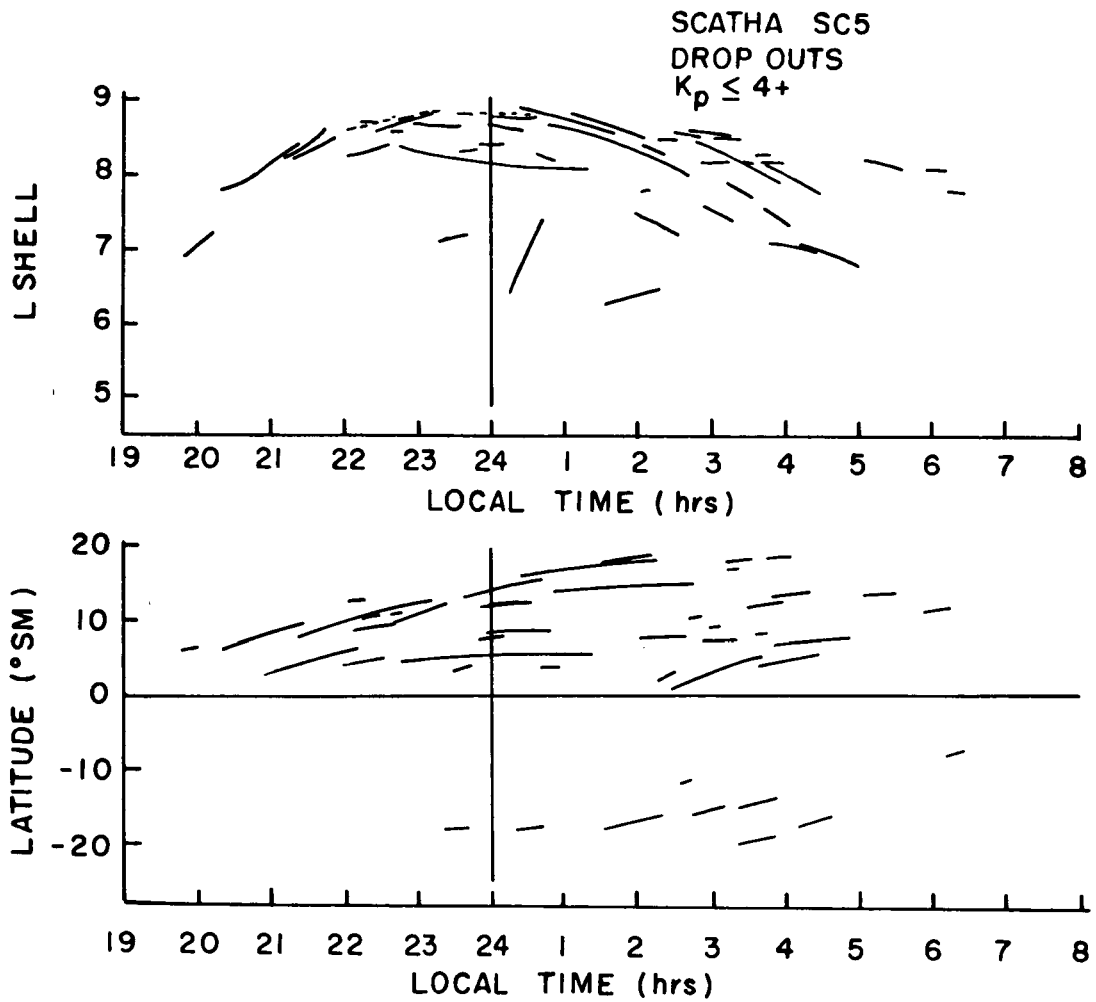


Figure 5. - SCATHA's position during dropouts for geomagnetically quiet days ( $K_p \leq 4+$ ).

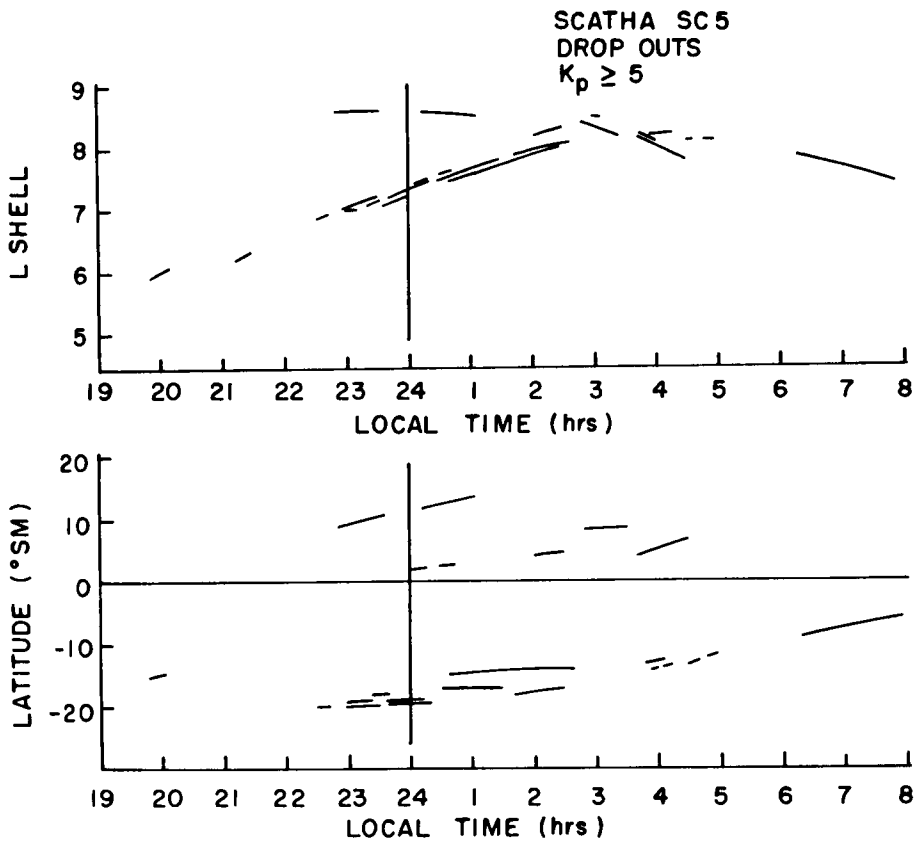


Figure 6. - SCATHA's position during dropouts for geomagnetically disturbed days ( $K_p > 4+$ ).

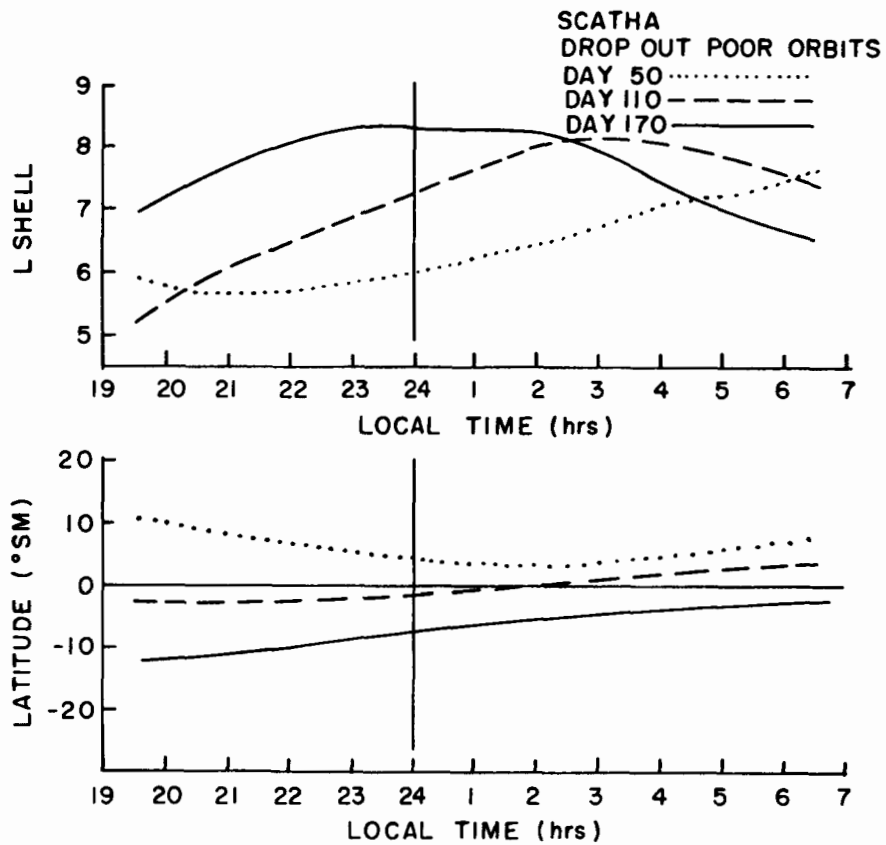


Figure 7. - SCATHA's orbits during the three dropout poor periods evident in Figure 4.